EXPERIMENTAL STUDIES
ON THE
LIMIT ANALYSIS OF
REINFORCED CONCRETE FIXED-ENDED T-BEAMS

By

Kenneth Harold Murray

Thesis submitted to the Graduate Faculty of the
Virginia Polytechnic Institute
in candidacy for the degree of
Master of Science
in
Structural Engineering

APPROVED:

Chairman, Dr. R. M. Barker

Dr. G. A. Grey

Dr. H. M. Morris

Dr. R. H. Myers

October 18, 1966

Blacksburg, Virginia

TABLE OF CONTENTS

LIST OF FIGURES

LIST OF TABLES

I. INTRODUCTION

Limit design in reinforced concrete is of major interest to a number of researchers in structural engineering. Limit design, like plastic design in steel, is a technique in which more of the load-carrying capacity of structural members may be utilized. This design then comes closer to defining the actual collapse load than any of the previous design techniques, but since it does approximate collapse more closely, the theory is more difficult. To use this limit design, an easier method of limit analysis must be found.

The approach used in this research was to test a single-span fixed-ended T-beam loaded with concentrated loads at the quarter points until collapse occurred and to compare the results with the analytical predictions. Also obtained from the test will be moment-curvature relations which are needed in most limit analysis techniques.

Consider first some background information on the moment-curvature curve for reinforced concrete. Figure 1 shows the actual moment-curvature curve and the idealized trilinear curve for an example beam. The first straight line portion is the elastic region; the second, the strain hardening region; and the third, the strain softening region or descending branch. This curve is for an under-reinforced section; a necessary condition to get sufficient rotational

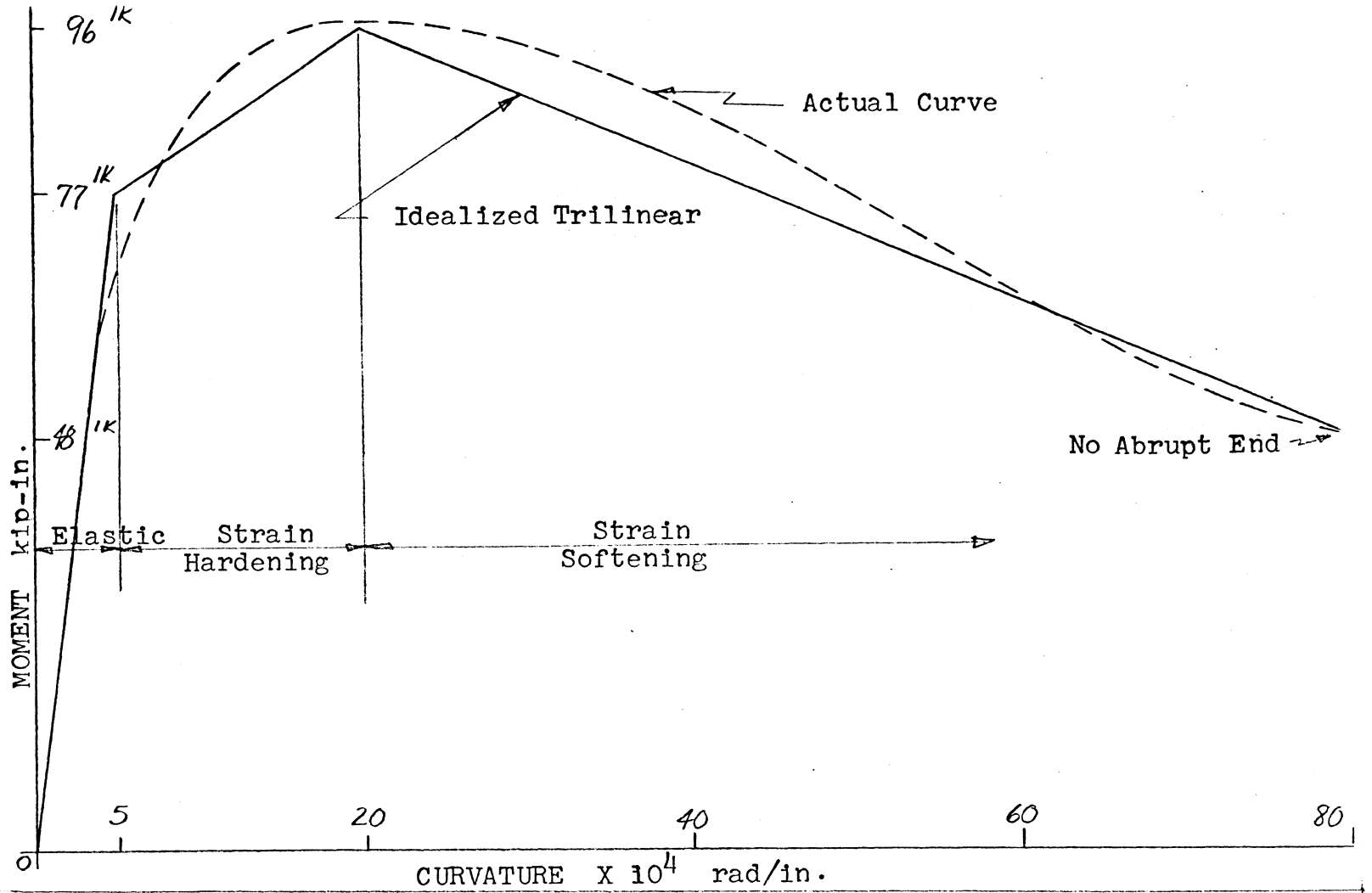

Figure 1. General Moment-Curvature Curve

capacity to make limit design effective. This under-reinforced condition is consistent with the present American Concrete Institute (ACI) Building Code.

As an example of limit analysis, consider a fixed-ended beam as shown in Figure 2, loaded at the third points. Comparing the different stages of analysis, we have:

A. Linear Analysis: The elastic moment diagram is shown in Figure 2 with M_A equal to 96 kip-feet and M_B equal to 48 kip-feet. The moment at A is at the ultimate value, therefore, causing the section to yield and a plastic hinge to form. In linear analysis, this would constitute failure. The load for this first and simplest case at failure is 24 kips. Note that the beam has not collapsed; it has only met the linear condition of failure.

B. Bilinear Analysis: Figure 3 shows this case and results. Using the first two portions of the idealized moment-curvature curve, moment redistribution takes place giving the new moment diagram shown. M_A is still 96, but M_B is now 60 kip-feet. We have assumed that all of the rotation at supports is taking place in a very small length which is an incorrect assumption, but still a better predicting

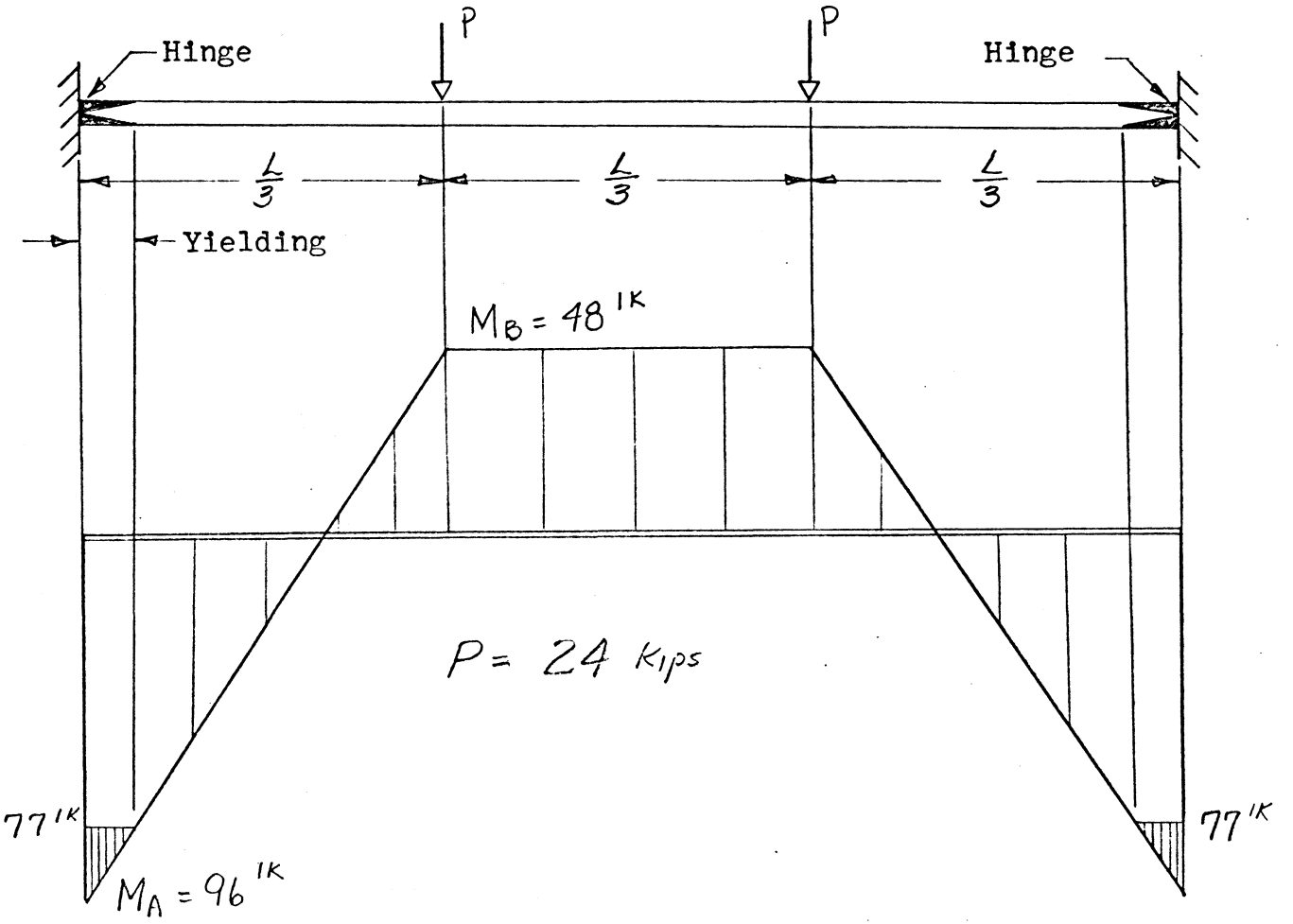

Figure 2. Fixed Ended Beam with Elastic Case Moment Diagram

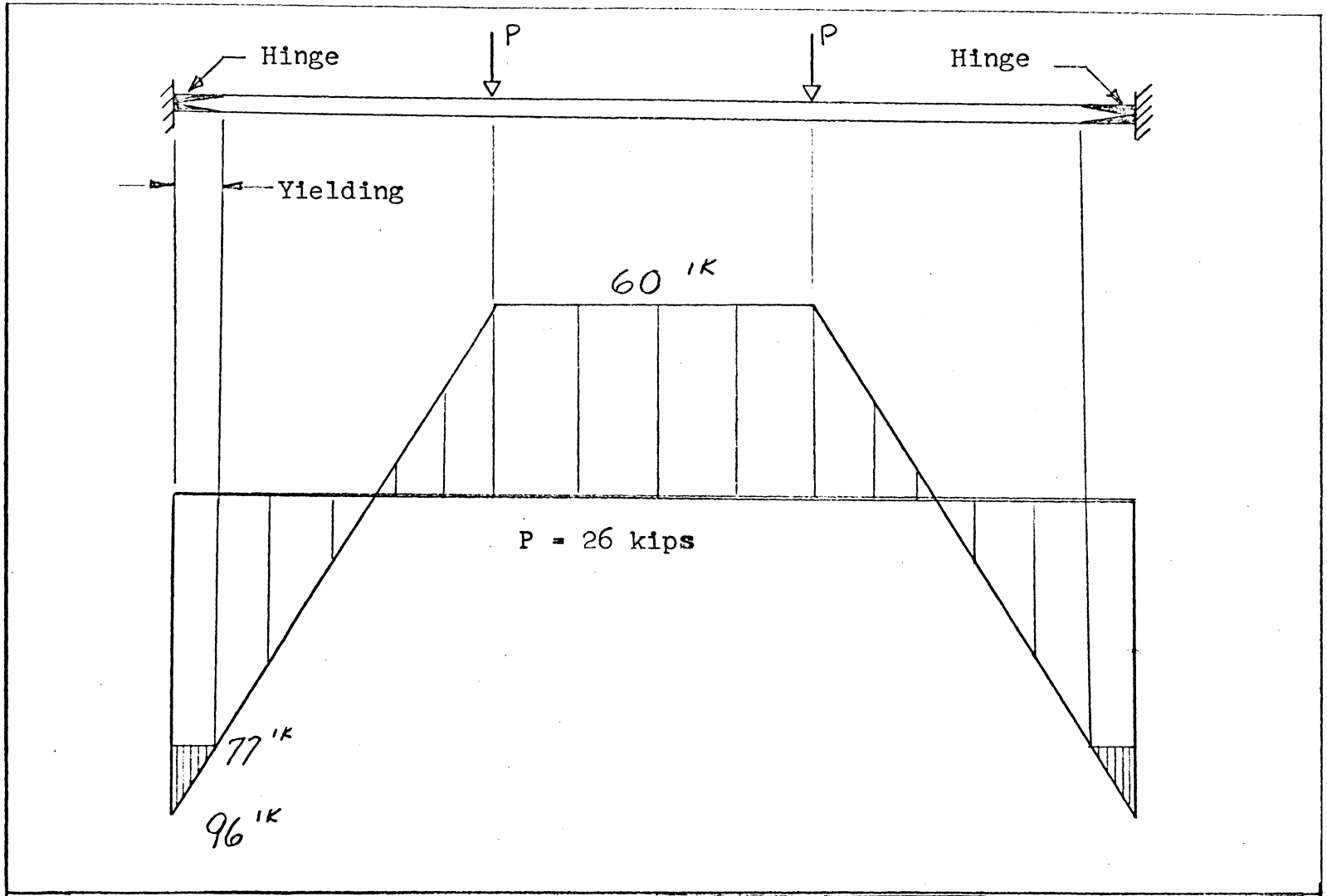

Figure 3. Moment Diagram for Bilinear Case

technique than the linear case. The failure load this time is 26 kips due to the moment redistribution.

C. Bilinear Analysis With Contamination Length: A length of d/2 is added to each hinge length. The added length is known as a contamination length and is defined as the length along the beam that the plastic hinge spreads beyond the theorical length. This contamination length is caused in part by the spread of yielding in the steel which has been observed by other researchers(8, 9, 10, 11). The d/2 factor is the best estimate available for the contamination length. This additional length to the plastic hinge increases the rotation capacity at that section. This additional rotation allows more moment to redistribute and, therefore, raises the calculated collapse load. Figure 4 shows the results of this analysis which has M_A equal to 96, M_B equal to 78 kip feet, and P equal to 29 kips.

In Figure 5 the three different analyses techniques are shown together in order to emphasize the additional load capacity obtained by using more of the moment-curvature curve in the analysis. The linear case is shown at the top,

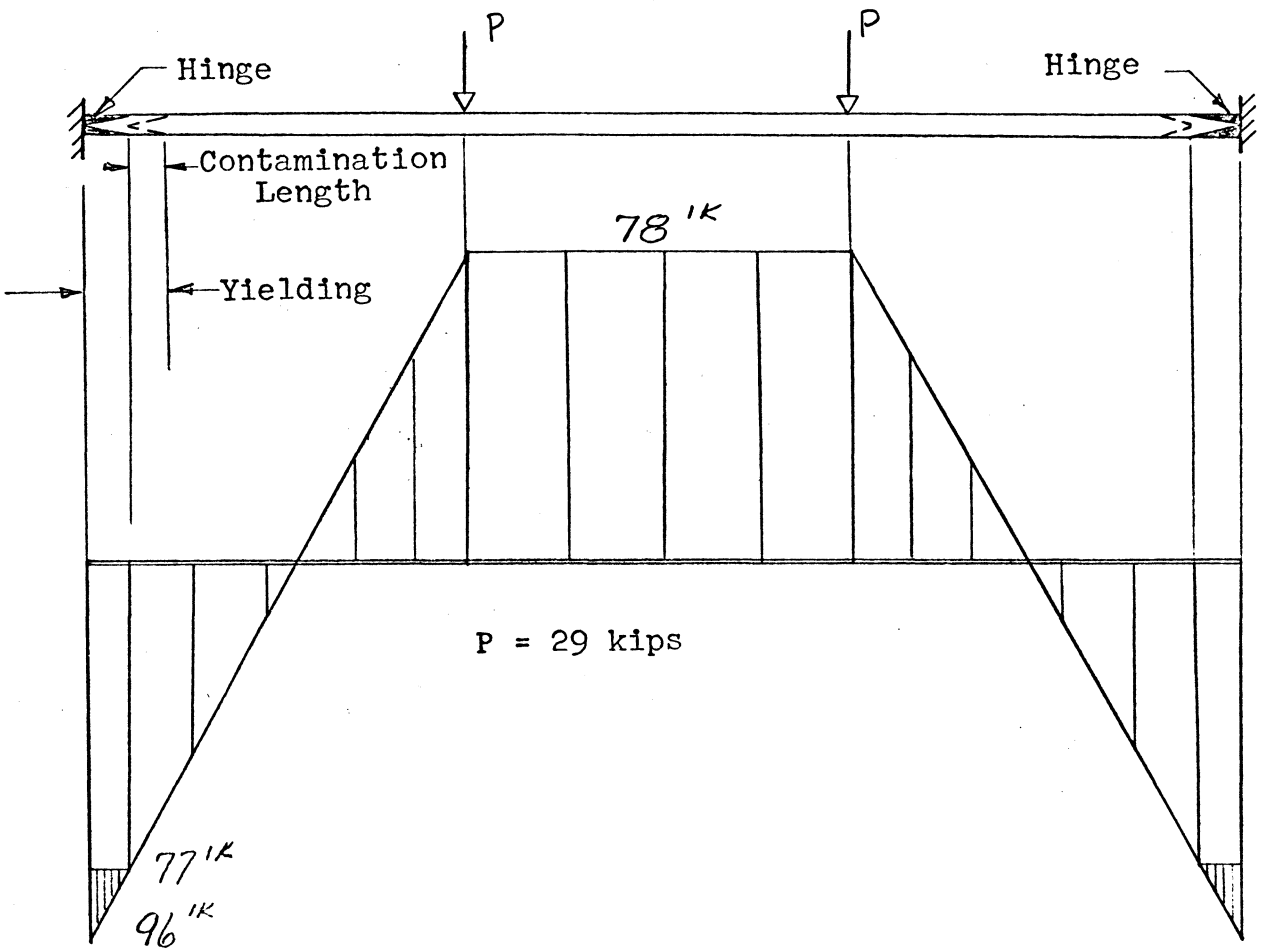

Figure 4. Moment Diagram for Bilinear Case with Contamination Length

and the others in order of presentation down to the final case, using the bilinear curve and a contamination length.

The question to be answered in this investigation is, "Does reinforced concrete have sufficient rotational capacity to make limit analysis applicable in design problems?" This investigation used a T-beam on simple supports with cantilever ends. Steel percentages were varied at the supports in order to determine the effect of the steel percentage on the rotational capacity of a reinforced concrete section.

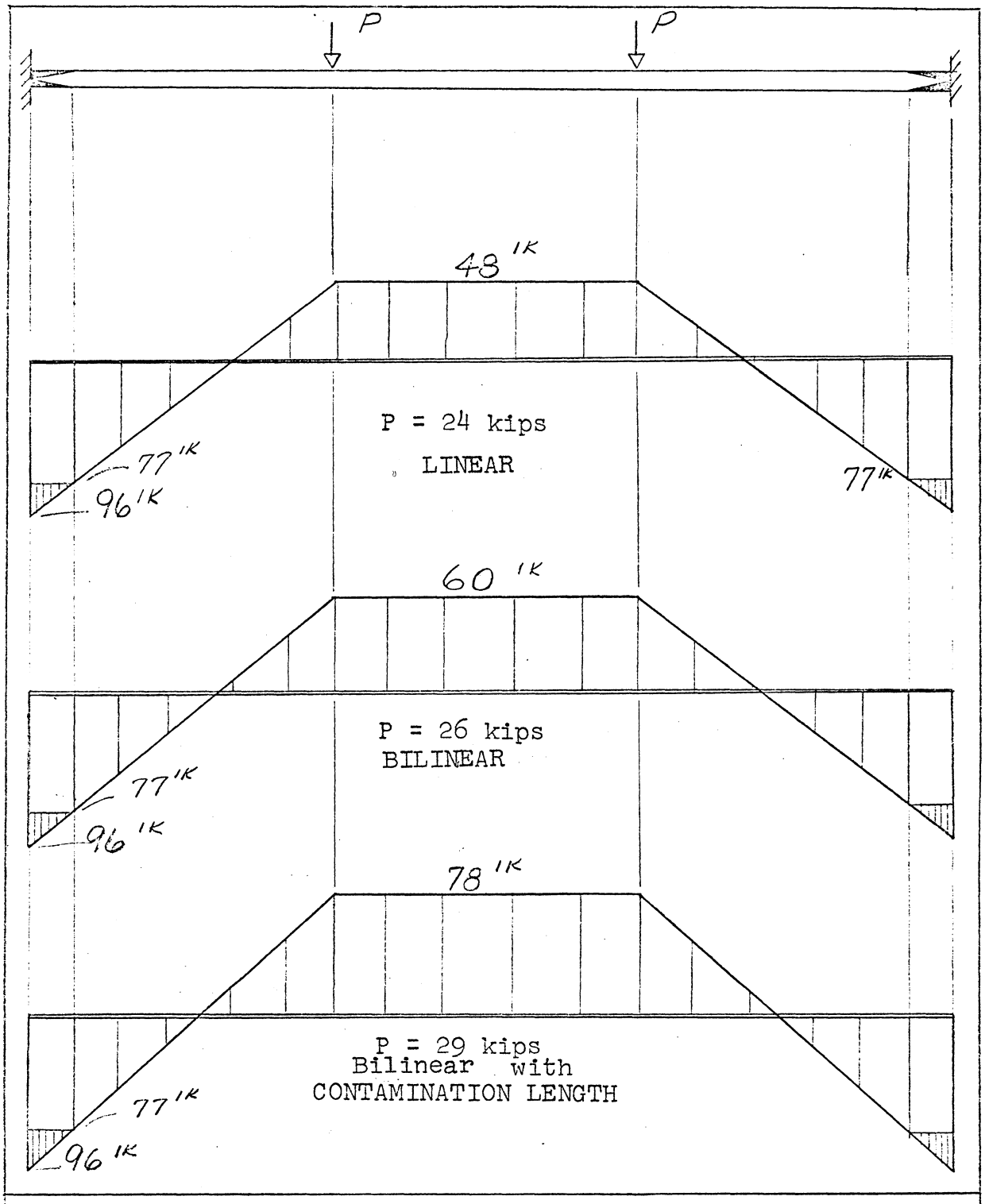

Figure 5. Comparison of Moment Diagrams

II. REVIEW OF LITERATURE

Baker[1] began the study of the rotational capacity of reinforced concrete members in 1949 and made the following statements at the conclusion of his first investigation:
(a) plasticity of concrete considerably increases the ultimate resisting moment of reinforced concrete beams;
(b) yield of reinforcement can provide advantageous moment redistribution.

In 1955, Chan[2] published the results of his Ph.D. work on the ultimate load method of designing statically indeterminate structures. His experimental work was divided into two parts: (a) seven beams, reinforced for both tension and compression with mild steel, which were six inches deep, 3-5/8 inches wide, and 52 inches in span, were subjected to combined axial compression and mid-span loading; (b) sixteen 12-inch long specimens, either prisms six inches square or cylinders six inches in diameter, with closely spaced stirrups, were eccentrically compressed. He concluded from these tests that concrete bound properly could deform enough to allow large rotations to occur. He describes the available rotation with this expression:

$$\theta_p = \int_0^{h_1 z} M\left(\frac{1}{EI_u} - \frac{1}{EI_e}\right) ds$$

Where

$$h_l z = \int_{M_y}^{M_u} \frac{dM}{dM/dz}$$ plastic hinge length

θ_p = available rotation

EI_u = the plastic value of EI

EI_e = the elastic value of EI

His investigation also included studying the length of the plastic hinge and its influence on rotational capacity. He concluded that, even if one assumes that all rotation occurs at a point, only a maximum (conservative) error of six percent arises which can be considered insignificant.

In 1960, Wright and Berwanger[3] reported their results of tests on eight reinforced concrete beams. Two were simply supported, single span beams while the other six were symetrical beams continuous over two spans. The cross section of the beams was constant at 3 inches by $6\frac{1}{2}$ inches with a span length of four feet. Parameters studied were tension and compression steel percentages which varied from 0.7 to 3.52. They derived the following simplified equations for rotational capacity:

1. With tension steel only

$$\Phi_{max}/\Phi_y = 1/4q_y^2$$

2. With both tension and compression steel

$$\Phi_{max}/\Phi_y = 1/5q_y q'_u$$

Where

ϕ_{max} = rotation at collapse

$\phi_y = \frac{M_y}{EI}$ = rotation at yield

M_y = moment at yield

q_y = pf_y/f'_c

p = percentage of tension steel

f_y = yield stress of tension steel

f'_c = compressive strength of concrete

q'_u = $\frac{pf_{su} - p'f_y}{f'_c}$

p' = percentage of compression steel

f_{su} = stress in tension steel at collapse

f'_y = yield stress of compression steel

This equation was verified by their test results.

In 1962, Chan[4] described the results of an investigation of 67 beam and column tests. The parameters studied were concrete strength from 2385 to 6385 psi, percentage of tension reinforcement from 0.68 to 2.62, and percentage of compressive reinforcement from 0.35 to 4.08. He concluded from these tests that, although the ultimate strain in concrete varies, it may be considered a constant when designing, and that given a moment distribution, the rotational capacity varies inversely with the depth to the

neutral axis. It was shown analytically, and verified experimentally, that the rotational capacity could be increased by the addition of short lengths of compression steel at the hinging section. This compression steel did not affect the moment capacity while increasing the rotational capacity. An alternate method was also described to obtain higher rotations. This method used closely spaced binders or stirrups at the hinging region.

In July, 1964, Pfrange, Siess and Sozen[5] published in the Journal of the ACI their findings concerning the effect of the steel percentage on the rotational capacity of reinforced concrete beams. Their tests were conducted on rectangular cross sections with the following variables:

1. p - percentage of tension reinforcement which had the values of 1, 2, 4, and 6.
2. d'/t - the cover to total depth ratio which had values of 0.05, 0.10, and 0.15 inches.

From these tests they concluded that increasing the ratio of reinforcement decidedly stiffens the section against rotation.

In November, 1964, the American Concrete Institute and the American Society of Civil Engineers jointly held an "International Symposium on the Flexural Mechanics of Reinforced Concrete." At the symposium, the leading researchers in the field gathered and presented their

individual findings on the flexural mechanics of reinforced concrete. Sawyer[6] began by listing the areas of research which have been studied, and also discussing others which need to be studied.

Of interest to this author were the papers by Barnard[7], Rosenblueth and de Cossio[8], Sawyer[9] and Mattock[10].

Barnard's[7] purpose was to explain the flexural behavior of statically indeterminate reinforced concrete beams when loaded to collapse. He explained that moment can be falling off at one section while the total load is increasing, and that this will continue until the energy balance ceases to be satisfied. When the external energy increases beyond the internal resistance, the beams collapse.

Rosenblueth and de Cossio[8] presented their work on instability failures of reinforced concrete sections using the descending branch of the force-deformation curve. A method based on a moment rotation approach with an assumed contamination zone is also discussed.

Sawyer[9] derived the required moment curvature relationships and plasticity factors and presented them quantitatively to be used in design. His equation for ultimate concrete curvature is:

$$\Phi_u = \epsilon_c/(A_s f_y/.85 f'_c k_1 b)$$

Where

Φ_u = ultimate concrete curvature

ϵ_c = ultimate concrete strain (0.0038)

A_s = steel area

f_y = steel yield stress

k_1 = concrete strength factor (0.85)

f'_c = ultimate concrete stress

b = width of compression face.

The design procedure is outlined based on these quantities and revisions in present load factors are recommended, based on both a critical re-examination of simple beam test results and special characteristics of bilinear analysis. This design procedure is verified by tests of other researches on continuous beams.

Mattock's[10] paper reports the results of tests on 37 beams with the following parameters:

1. f'_c, concrete strength varied from 4000 to 6000 psi
2. f_y, steel yield strength varied from 47 to 60 psi
3. d, effective depth varied from 10 to 20 inches
4. L, span length varied from 55 to 220 inches
5. p, percentage of steel varied from 1 to 3.

Among his conclusions were the following:

1. If the maximum concrete compressive strain is assumed as 0.003 in./in., then the calculated ultimate strength and curvature values will be

underestimated. The actual values of concrete compressive strain will be greater than the usually assumed 0.003 in./in.

2. If strain hardening of the reinforcement and variation of maximum concrete compressive strain with shear are considered, then equations derived from well-known principles of equilibrium of forces and compatibility of strains can be used to obtain close estimates of the moments as well as safe estimates of curvature and rotations occurring at sections of maximum moment.

3. The spread of plasticity away from the section of maximum moment is directly proportional to the ratio z/d and inversely proportional to the net tension reinforcement $(q-q')/q_b$. He derived the following equation for the ratio of the total inelastic rotation in length z to the inelastic rotation in length d/z:

$$\frac{\theta_{tu}}{\theta_u} = 1 + \left[1.14\sqrt{\frac{z}{d}} - 1\right]\left[1 - \left(\frac{q-q'}{q_b}\right)\sqrt{\frac{d}{16.2}}\right]$$

Where

θ_{tu} = total inelastic rotation occurring between the section of maximum moment and adjacent section of zero moment

θ_u = inelastic rotation occurring within a length of half the depth to one

side of the section of maximum moment

d = effective depth

q = tension reinforcement index pf_y/f'_c

q' = compressive reinforcement index $p'f'_y/f'_c$

q_b = reinforcement index for balanced ultimate strength conditions

z = distance from section of maximum moment to an adjacent section of zero moment.

This equation can be used to predict a reasonable and safe limiting value for the inelastic rotation in the hinging region.

III. THE INVESTIGATION

A. Theoretical Analysis of Beam Tested

One theory now considered for the inelastic analysis of indeterminate reinforced concrete structures was presented by Rosenblueth and de Cossio[8] and Sawyer[9] in their papers given at the International Symposium on Flexural Mechanics of Reinforced Concrete. Sawyer's method of predicting the moment-curvature curve and Rosenblueth and de Cossio's method of balancing rotations were used in evaluating the ultimate load for Beam No. 1.

Figure 6 shows the moment-curvature curves which were generated by Sawyer's method using the following parameter values:

Section A-A (support)	Section B-B (middle)
$p = 0.016$	$p = 0.00516$
$p' = 0.026$	$q = 0.0686$
$q = 0.251$	$k_p = 125$
$q' = 0.409$	$K_e = 430{,}000$ kips-sq. in.
$k_p = 120$	$K_p = 3440$ kips-sq. in.
$K_e = 265{,}000$ kips-sq. in.	
$K_p = 2210$ kips-sq. in.	

The ACI Code was followed in determining the ultimate moments for both sections with the strength reduction factor (ϕ) not being used.

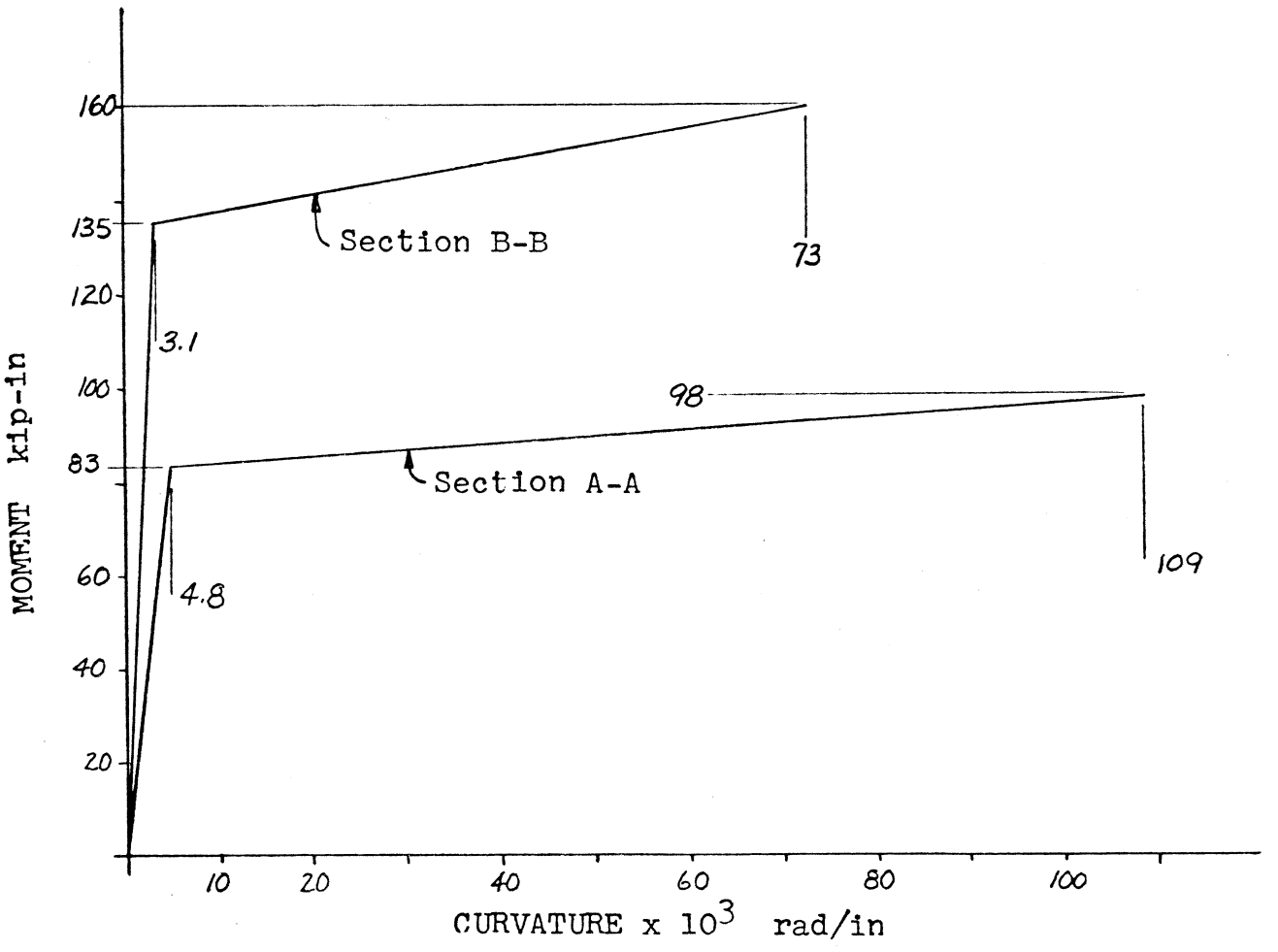

Figure 6. Theoretical Moment-Curvature Curves For Beam No. 1

Figure 7 gives information on the loading system, the moment diagram, and the curvature diagram. The curvature diagram follows the outline set by Rosenblueth and de Cossio.

The following equations were then used to determine the ultimate load:

1. $M_1 + M_3 = 48P$, $(M_1 \quad M_{u1})$
2. $M_3 - M_2 = 12P$, $(M_3 \quad M_{u3})$
3. $X = 32 - 2M_3/3P$
4. $X_1 = 2(M_3 - 135)/P$
5. Positive rotation area = Negative rotation area. (From Figure 7, curvature diagram.)

It can be shown using equation (1) and the moment-curvature curves that the maximum value of P is 5.4 kips. Considering this, 5.4 was used in the equilibrium equations (1) through (4) which were then substituted into the compatibility equation (5) in terms of M_3. Solving for M_3 proved tedious, but it was found that M_3 was greater than its ultimate value which cannot be true; therefore, P was known to be less than 5.4. After considering the matter, M_1 was set at its ultimate value and M_3 was found to be equal to 143 kip-inches, which is below its ultimate value and, therefore, reasonable. The value for P with $M_1 = 100$ and $M_3 = 143$ is 5.06 kips.

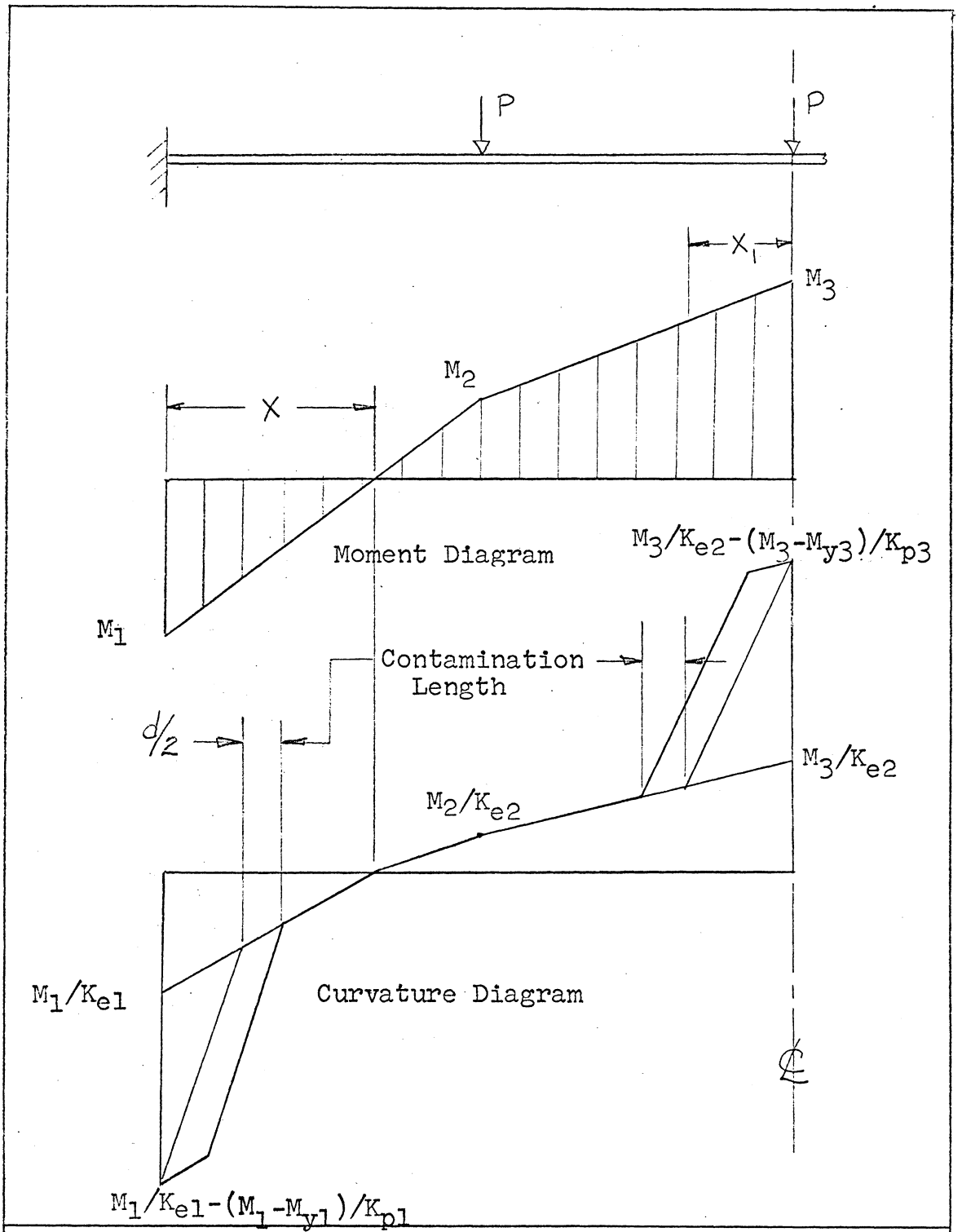

Figure 7. Moment and Curvature Diagrams

B. Experimental Work

Three beams were tested with cross section dimensions as shown in Figure 8. Each beam had a span length of eight feet and cantilever ends of two feet six inches. These beams varied in tension steel only. All important properties of each beam are given in Table 1. All steel reinforcing was ASTM-A-305 deformed intermediate grade steel except stirrup steel which was hot-rolled, quarter-inch round, smooth bars.

The concrete used was mixed in a commercial $3\frac{1}{2}$ cubic foot mixer. A batch of concrete was approximately $2\frac{1}{2}$ cubic feet with three batches required per beam. Care was exercised in the mixing of each batch to obtain the needed uniformity in concrete strength. The concrete strength, for which the author aimed, was 3000 psi with a slump of about $3\frac{1}{2}$ to 5 inches. The concrete contained the following quantities per cubic yard:

Portland Cement (Type III)	507 pounds
Sand	1,565 pounds
Coarse Aggregate (3/4 maximum size)	1,650 pounds
Water (approximately)	316 pounds

Two test cylinders were made from each batch.

The T-beams were cast in forms fabricated of 3/4 inch plywood. Care was taken to varnish and oil the forms before each beam was poured. This precaution proved beneficial and the forms were removed assembled. As a

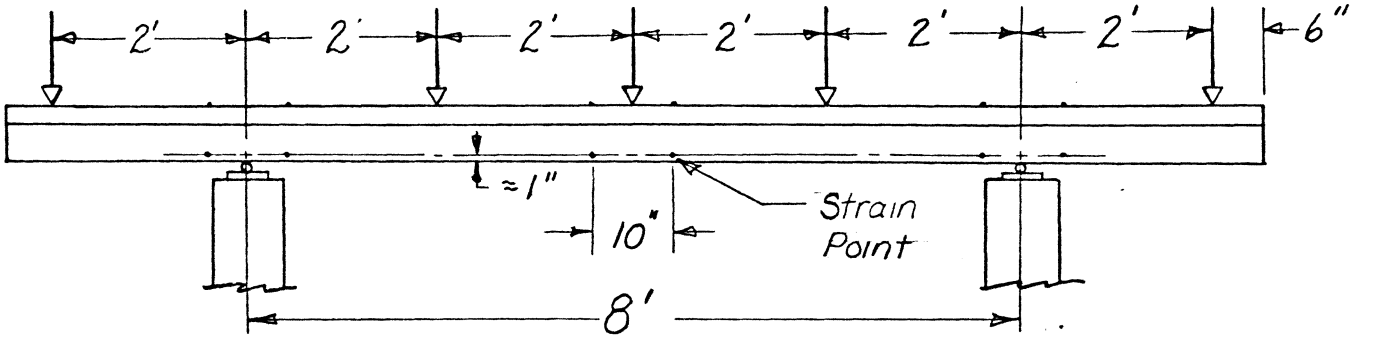

LOCATION OF STRAIN POINTS

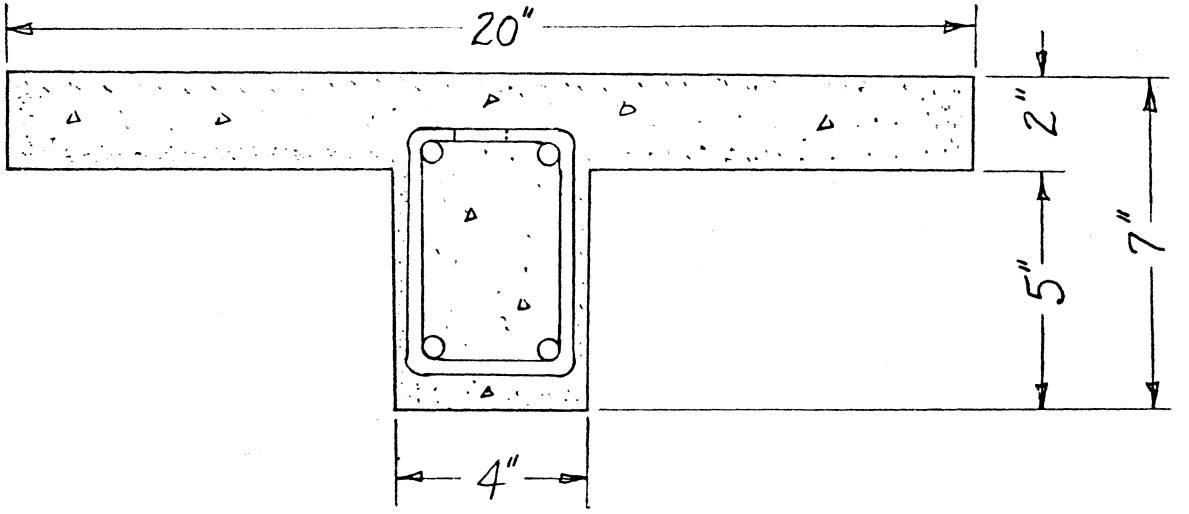

CROSS SECTION

Figure 8. Location of Strain Points and Cross Section Dimensions

TABLE 1

Properties of Beams

Property	Beam 1	Beam 2	Beam 3
Effective Depth	6.000 in.	5.938 in.	5.875 in.
Tension Steel Mid-Span	2 No. 5 (0.61 sq. in.)	2 No. 5 (0.61 sq. in.)	2 No. 5 (0.61 sq. in.)
Tension Steel At Support	2 No. 4 (0.39 sq. in.)	2 No. 5 (0.61 sq. in.)	2 No. 6 (0.88 sq. in.)
Compression Steel At Support	2 No. 5 (0.61 sq. in.)	2 No. 5 (0.61 sq. in.)	2 No. 5 (0.61 sq. in.)
Concrete Strength At Mid-Span (Avg. 2-cylinders)	3975 psi	3480 psi	3040 psi
Concrete Strength at Right Support (Avg. 2-cylinders)	3690 psi	3480 psi	2900 psi
Concrete Strength at Left Support (Avg. 2-cylinders)	3790 psi	3430 psi	3170 psi

result of this, dimensional variation between beams was reduced.

Curing of each beam was, due to location and size of the beams, handled by applying wet burlap immediately after casting and re-wetting each day for two days. The beams were then allowed to dry with the burlap still in place for two additional days, at which time the beam was removed from the forms. On the seventh day, in each case, the beam was placed on the supports and made ready for the test on the following day. Concrete cylinders were handled in the same manner, and the results of the compression tests run on the same day as the beam was tested are given in Table 1.

The first problem encountered was the measuring of ultimate strains in both the concrete and the steel. A special strain gage was designed by Dr. R. M. Barker and the author, and fabricated by the technician in the Civil Engineering Department. A sketch of this gage is shown in Figure 9. The gage simply measures the relative distance between two points, which is compared to the reading at another load stage to give the strain.

Special brass plugs were formed into the concrete at the points where strain readings were needed. These plugs were located 10 inches apart by aluminum strips placed on top of the concrete during pouring. Points on the side were placed by screws through the form.

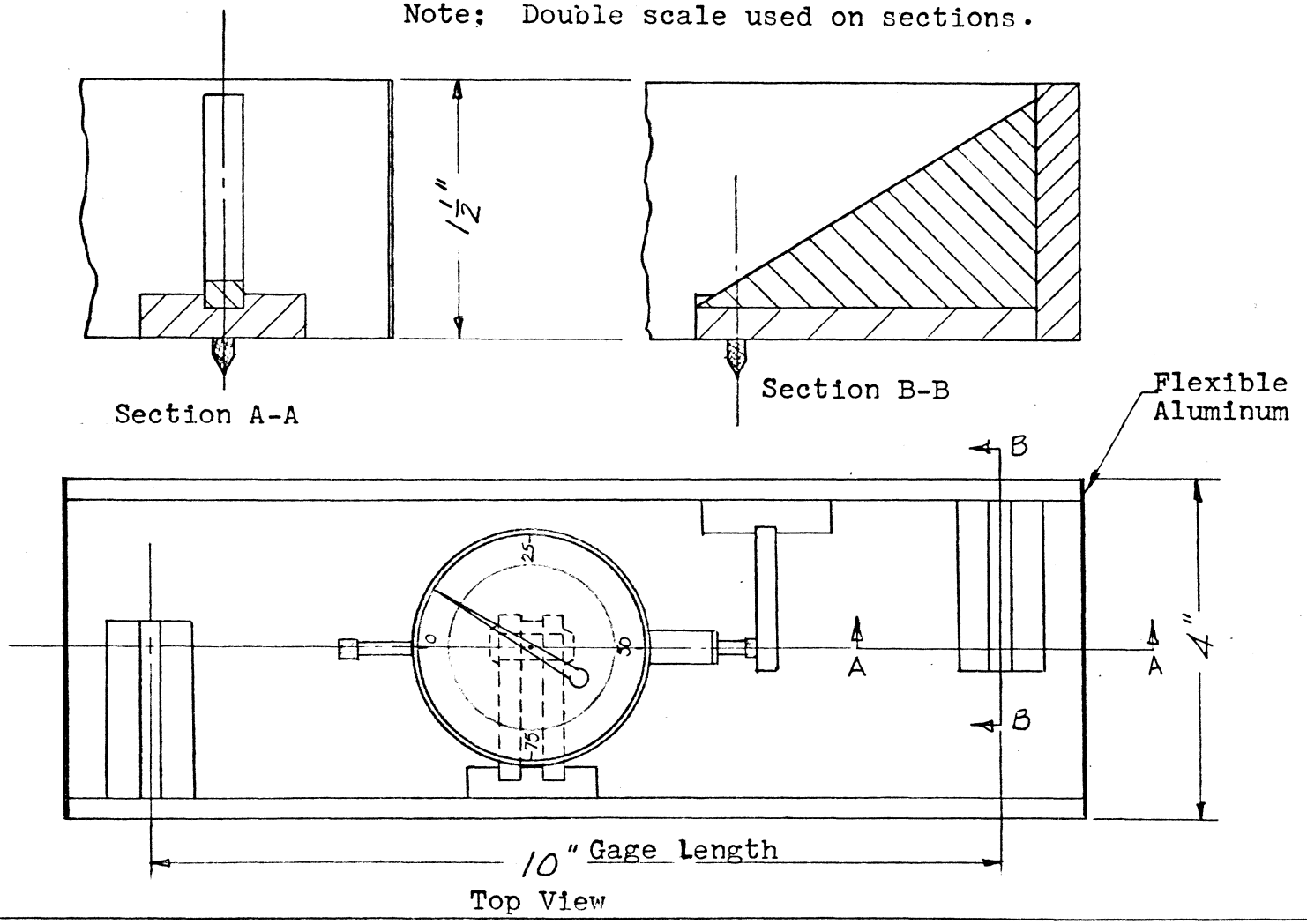

Figure 9. Strain Gage

Just prior to testing, the plugs were capped with a screw-in type cap having a 1/32 inch hole. The hole was the same size as the points on the strain gage. This combination gave very good results and was accurate to ± 0.002 inch. This accuracy was sufficient considering the range of strain over which the gage must read.

The locations of the strain points are shown in Figure 8. Points on top were on the surface and measured the strain there. Points on the side were placed as close as possible to the centroid of the bottom steel.

The loading system consisted of five hydraulic jacks anchored to the test floor, which pulled downward on the beam. Eye-bars anchored the jacks to the testing floor, and one-inch round bars were formed into the beam to attach the jacks so the load could be applied at the center of the beam to eliminate twisting.

Five jacks were selected at random and then calibrated using a standard testing machine in the Engineering Mechanics Laboratory. A statistical analysis was run to determine which three jacks had the same slope on the pressure-load curve. Three were selected and marked to be used on the same pressure line.

The loads were applied by the jacks at the quarter points, two feet apart, and at two feet from the support on the cantilever. The loads on the simple span were on the

same pressure line with the equal slope jacks. Each cantilever jack was on a separate line, and all the jacks were calibrated so that the load could be calculated from the pressure on the jack.

The cantilever loads were adjusted to maintain a zero slope at the top surface of the beam. The slope was determined by a four-inch level vial placed on a pad of mortar and leveled with all dead load on the beam.

Pressure was applied by a three-gallon-per-minute pump powered by an electric motor. These were mounted on a test stand with pressure gages on each line as well as on the system. The line pressures were adjusted by using brake valves with screw handles to vary the pressure.

Figure 10 shows the complete setup during a test.

Each test began early in the morning with an initial load being applied. To follow precedence, a 15-minute waiting period was observed before strain readings were taken. Load increments were four at 15 percent of yield load, and eight at five percent with the remaining increments after yield load being controlled by deflection. These last increments were taken at 0.200 inch increases in center line deflection. The test ran approximately seven hours continuously before collapse of the beam.

C. Results

The test results were all similar in certain respects as will be shown. Tension cracks at the supports

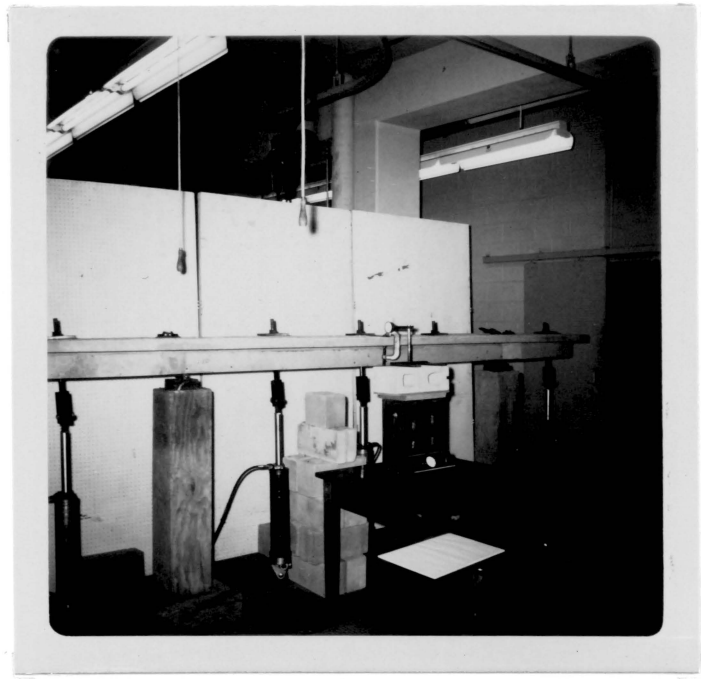

Figure 10. Complete Test Setup

occurred at about 45 percent of ultimate load in all cases. Tension cracks at the center section were usually found at about this same level of load. The crack pattern at the support was the same in all cases with all the cracks running toward the roller. This pattern looked like a "V" since the cracks were spread wide at the top, but closed up at the bottom. Center cracking is best shown in Figure 11. Cracking was concentrated at the center at low loads, but spread along the beam as the load increased. Figure 12 shows total picture of cracking.

Beam No. 1, in contrast to the others, failed at the center section as was expected. Yield moments were present at the supports and the center. The support sections rotated sufficiently to allow a hinge to form in the center which caused an instability failure. The center section failed in compression since the section was under-reinforced. A large section of the flange completely separated from the stem and fell. Both support sections were still carrying maximum or near maximum moment.

Beams No. 2 and No. 3 acted essentially in the same manner; both failed at the support section without a hinge forming in the center section. In each case, the failure of the support section was caused by a combination of shear and moment which can be seen in Figure 13 and 14. Figure 13 shows the failure of the support section in Beam No. 2, while Figure 14 shows the same section on Beam No. 3. During the

Figure 11. Center Crack Pattern

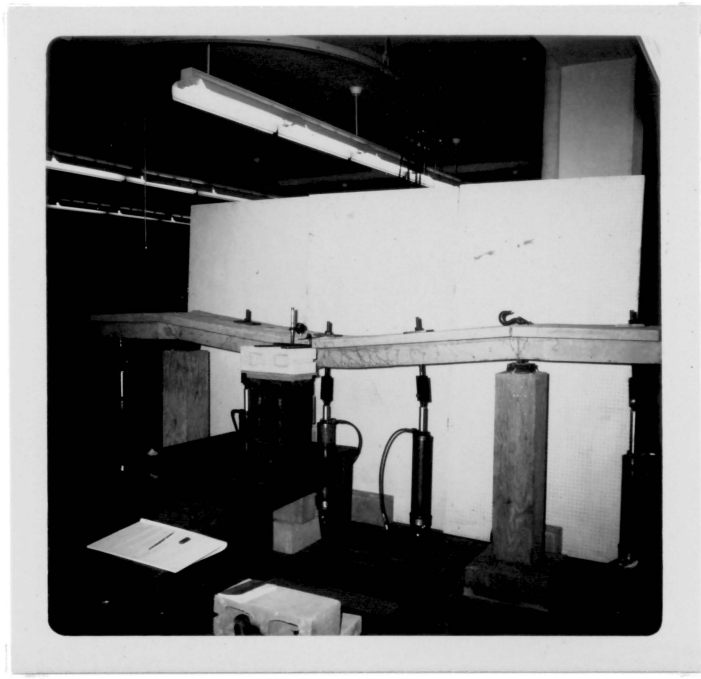

Figure 12. Total Crack Pattern

Figure 13. Appearance of Failed Support Section, Beam No. 2

Figure 14. Appearance of Failed Support Section, Beam No. 3

sudden failure of the support section, an unusual crack formed on the top, as shown in Figure 15. This crack ran longitudinally along the beam approximately in the center of the stem and turned at a right angle spreading transversely across the flange. The transverse section was at the end of the top steel extended from the support section.

The data obtained from the experiments were fed into a computer program and reduced to the form presented in Tables 2, 3, 4, 5, 6, 7, 8, 9, and 10 found in Appendix A. The computer program can be found in Appendix B.

From these results, graphs were plotted to emphasize more clearly the findings of this investigation. Figure 16 is a plot of moment versus curvature for the center section. All data points were used from each test since the section properties were essentially constant. The curve shown is not necessarily the best fitting line but shows the large rotation capacity of the section. Although each beam followed the same curve, each did not rotate the same amount. These cut-off points are noted on the curve.

Figure 17 is a plot of moment versus curvature for the support section with all three beams shown. These curves show the effect of the steel percentage on the moment-curvature curve.

Figure 18 is a non-dimensional plot of moment divided by the maximum value taken from Figure 16 versus

curvature. This plot also shows the different rotational capacities of the three beams.

Figure 15. Support Crack Pattern on Top Surface

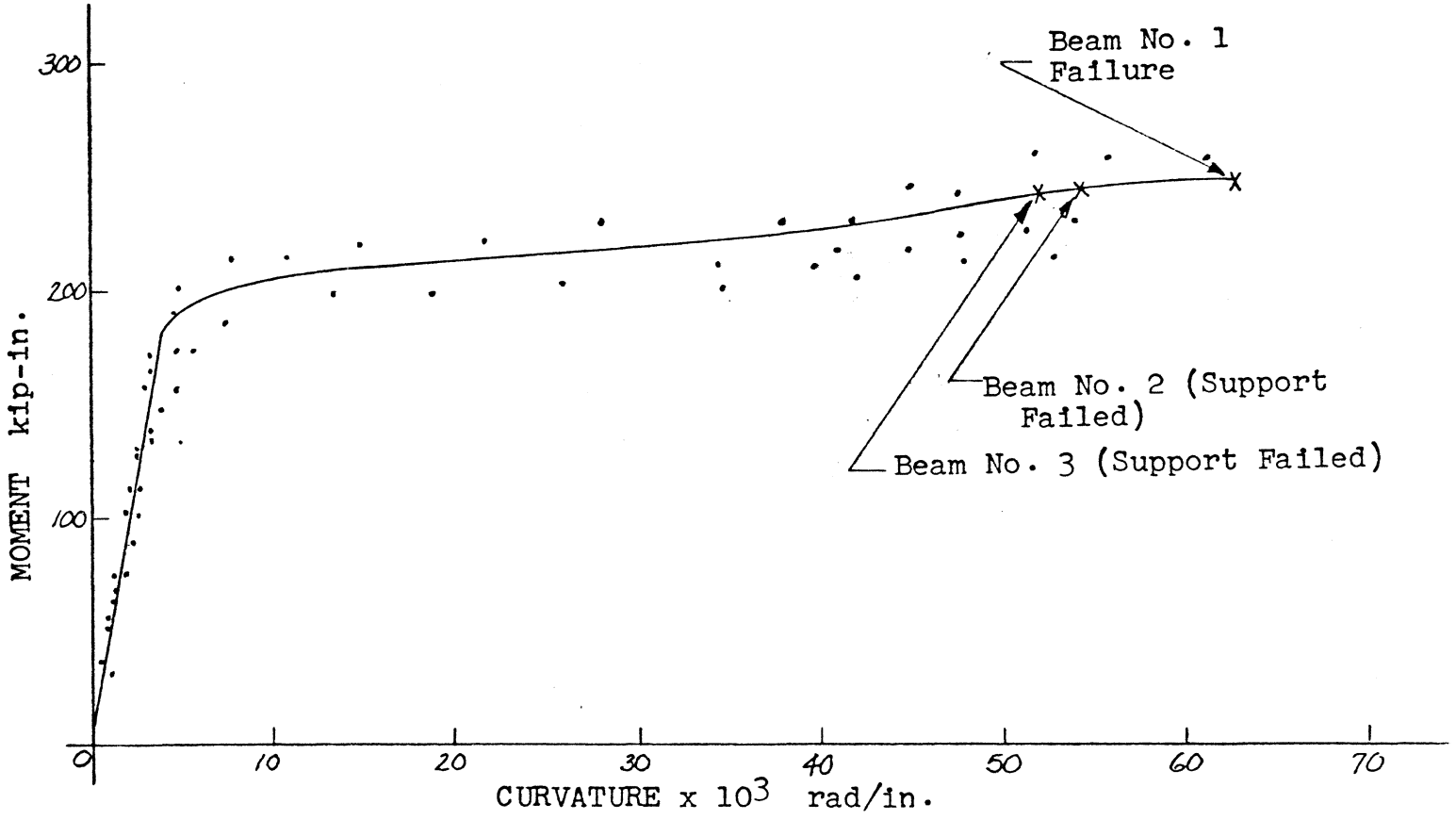

Figure 16. Moment-Curvature Curve, Center Section

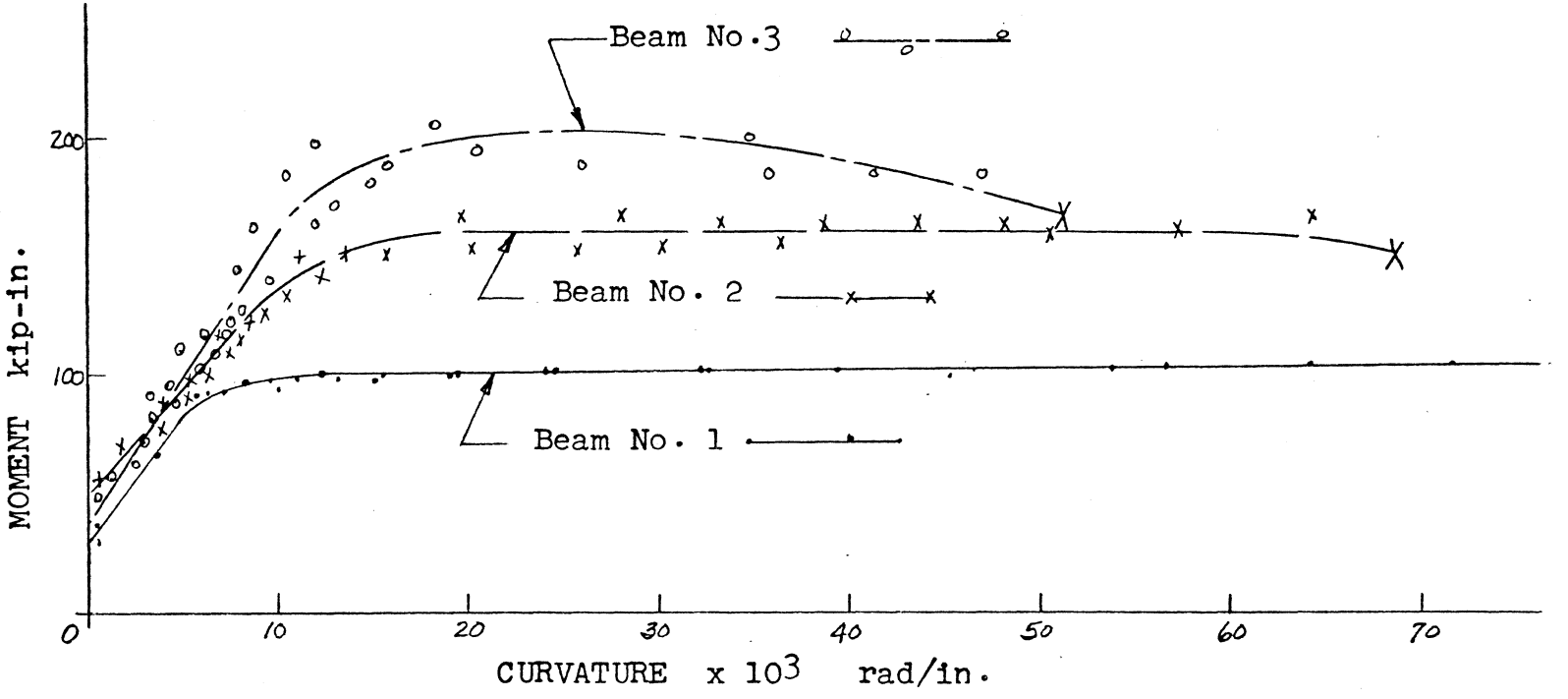

Figure 17. Moment-Curvature Curve, Support Sections

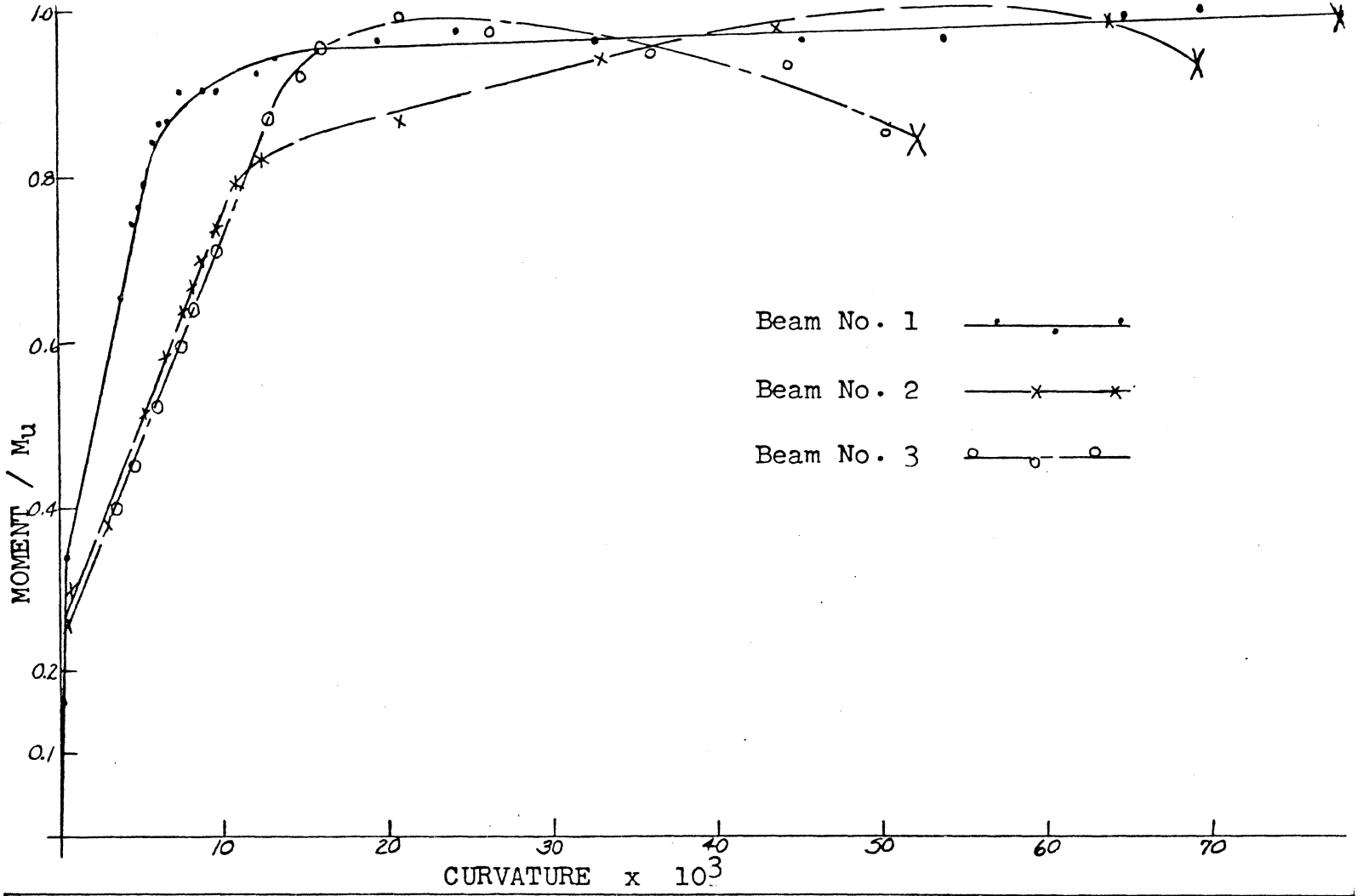

Figure 18. Non-Dimensional Moment-Curvature Curve, Support Sections

IV. DISCUSSION

The objective of this investigation was to determine if a reinforced concrete T-beam, with a reasonable steel percentage, is ductile enough to allow a mechanism to form before any section failed due to instability. Only Beam No. 1, using No. 4 bars as tension reinforcement at the supports, formed such a mechanism, but the question of whether the steel percentage was reasonable requires further evaluation. The steel percentage is 2.0, considering only the tension steel, but the net steel percentage, considering the compression steel, is negative since No. 5 bars were used as compression steel. The No. 5 bars in the compression zone are extensions of the positive steel in the center section as required by the ACI Code in Section 918 (f). This condition occurs in practice when designing continuous T-beams with large center section moments; therefore, it can be assumed that this steel situation is not unrealistic.

Beyond the major objective of this investigation were several areas of interest to the author concerning the action of reinforced concrete in bending to the point of collapse. These areas are found in Tables 2 through 10, which are direct from the computer. Each table contains values of (1) load, (2) moment, (3) rotation, (4) neutral axis depth, and (5) strain; Tables 3, 6, and 9 concerning

the center section also give values of center line deflection.

Upon careful examination, one can find values of rotation, neutral axis depth, and concrete strain which are negative or obviously in error. All of those errors occur at low loads. Strains are very small at low loads which present a problem for the mechanical strain gage used to measure them, since the small strains are lost in the accuracy of the gage. These gage readings, which are incorrect, are then used to calculate the neutral axis depth and strain.

There is also another point concerning the neutral axis depth, which needs to be discussed. During preliminary calculations of ultimate moment capacity using the ACI Code equations, a neutral axis depth at ultimate was calculated. This depth was in every case much smaller than the values shown in the tables of this thesis. This fact is due to the use of 0.003 in./in. for the ultimate strain in concrete by the Code in deriving its equations, since the ultimate strain experimentally was recorded much higher. This increase in strain will then lower the neutral axis.

Since the ultimate concrete strain has been mentioned, let us examine the experimental results. Considering only sections which actually failed and averaging, the value of concrete ultimate strain is 0.0083 in./in. If this is

compared with the standard of 0.003 in./in. set forth by the ACI Code in Section 1503 (c), an increase of 180 percent is observed. This increase is due mainly to the closely spaced stirrups at critical sections. The stirrups confined the concrete and caused a triaxial state of stress to form. This triaxial stress state increased the deformability of concrete.

In Figure 18, the non-dimensional plot of moment-curvature presents the conclusion that most researchers find, that by decreasing the steel percentage, the rotational capacity increases. Beam No. 1 seems to have a pure plastic curve; Beam No. 2 follows the usual curve with a strain hardening and softening region; Beam No. 3 shows no strain hardening, but only a strain softening region. It is difficult to make any definite statement about the relationship between steel percentage and rotational capacity, since compression steel was present in this investigation. The net steel index (q-q') is negative in No. 1, zero in No. 2, and positive in No. 3. If this is compared with Mattock's[10] statement in the discussion on his paper, there is some disagreement. Mattock says, "Complete redistribution of moment may probably be assumed to occur in continuous beams, provided the net tension reinforcement index at critical sections (q-q') is kept below about $0.5q_b$." From this investigation, (q-q') for all support sections was less than $0.5q_b$, but

only in one case did complete redistribution take place.

Looking at the "Theoretical Analysis" section, it is evident that the theoretical analysis is very conservative in its prediction of ultimate loads. ($P = 5.06$ kips, $P_{exp} = 7.50$ kips). The problem does not seem to be the moment-curvature curves, since they compare very well with those of this investigation. Some reasons for the 30 percent underestimation are as follows:

1. The ACI Code's equations for ultimate moment are conservative and therefore, when used, underestimate the quantity in question.
2. The contamination length at the support section was larger than the d/2 used.
3. Some needed additional rotational capacity could be used if the descending branch of the moment-curvature curve is considered in the analysis.

Looking closer at the first reason above, it was found that the reinforcing steel must have been in the strain hardening portion of its stress-strain curve. This has to be the case since the stress in the steel was approximately 70 si, while the yield stress was only 46.5 si. This could be a special situation occurring only with this particular lot of steel, but it does merit some attention in future investigations.

In regard to the third reason above, it was found that the descending portion of the moment-curvature curve was very difficult to obtain experimentally. This was due mainly to the inability to stop the beam from being destroyed by the momentum generated when the ultimate load was reached. Other investigators have solved this problem by using very stiff testing machines which slowly apply small deflections instead of using the normal testing machines.

V. CONCLUSIONS

After study of the results of this investigation, the following conclusions were made:

1. Ultimate concrete strain is greater than the ACI Code standard of 0.003 in./in. when confined in a beam with stirrup spacing governed by the ACI Code requirements. Tables 2 through 10.
2. The depth to the neutral axis remains approximately constant with increasing load, but there is a slight tendency to increase the compression zone of the concrete. Tables 2 through 10.
3. Some moment redistribution takes place with the steel percentage at the center section near balance and the support section net percentage less than half the balance percentage.
4. Rotational capacity increases with decreasing steel percentage. Figure 17.
5. Present theory using the bilinear moment-curvature curve with ACI Code ultimate moments is very conservative in its calculation of the collapse load.

ACKNOWLEDGEMENTS

The author would like to express his appreciation to Dr. Richard M. Barker of the Civil Engineering Department, Virginia Polytechnic Institute, for his suggestion of a topic worthy of investigation, and his leadership and guidance during the investigation and writing of this thesis.

Acknowledgement is made to NASA's Trainee Program which financed the author's graduate studies and other related expenses.

Acknowledgement is made to Dr. George A. Gray for his encouragement, and to Mr. Kenneth G. McCauley and his associates for their constant assistance in the laboratory.

Appreciation is also expressed to Professor Homer T. Hurst of the Agricultural Engineering Department for his assistance in obtaining testing equipment, and to the Civil Engineering Department for financial aid in purchasing the necessary materials for this investigation.

A special thanks is extended to my wife who typed this thesis and who gave me the necessary encouragement at home.

LITERATURE CITED

1. Baker, A. L. L., "A Plastic Theory of Design for Ordinary Reinforced and Prestressed Concrete Including Moment Re-Distribution in Continuous Members," Magazine of Concrete Research, No. 2, June, 1949, Pages 57-66.

2. Chan, W. W. L., "The Ultimate Strength and Deformation of Plastic Hinges in Reinforced Concrete Frameworks," Magazine of Concrete Research, Volume 7, No. 21, November, 1955, Pages 121-132.

3. Wright, D. T.; Berwanger, Carl, "Limit Design of Reinforced Concrete Beams," Journal of the Structural Division ASCE, Volume 86, No. ST7, Paper 2541, July, 1960, Pages 1-36.

4. Chan, W. W. L., "The Rotation of Reinforced Concrete Plastic Hinges at Ultimate Load," Magazine of Concrete Research, Volume 14, No. 41, July, 1962, Pages 63-71.

5. Pfrang, E. O.; Siess, C. P.; Sozen, M. A., "Load-Moment-Curvature Characteristics of Reinforced Concrete Cross Sections," Journal of the American Concrete Institute, July, 1964, Volume 61, No. 7, Pages 763-778.

6. Sawyer, H. A., Jr., "Status and Potentialities of Non-Linear Design of Concrete Frames," Flexural Mechanics of Reinforced Concrete - Proceedings of the International Symposium, Miami, Florida, November 10-12,

1964, Pages 7-28.

7. Barnard, P. R., "The Collapse of Reinforced Concrete Beams," Flexural Mechanics of Reinforced Concrete - Proceedings of the International Symposium, Miami, Florida, November 10-12, 1964, Pages 501-521.

8. Rosenblueth, Emilio; Diaz de Cossio, Roger, "Instability Consideration in Limit Design of Concrete Frames," Flexural Mechanics of Reinforced Concrete - Proceedings of the International Symposium, Miami, Florida, November 10-12, 1964, Pages 439-463.

9. Sawyer, H. A., Jr., "Design of Concrete Frames for Two Failure Stages," Flexural Mechanics of Reinforced Concrete - Proceedings of the International Symposium, Miami, Florida, November 10-12, 1964, Pages 405-439.

10. Mattock, A. H., "Rotational Capacity of Hinging Regions in Reinforced Concrete Beams," Flexural Mechanics of Reinforced Concrete - Proceedings of the International Symposium, Miami, Florida, November 10-12, 1964, Pages 143-182.

11. Nordell, W. J., "Plastic Hinge Formation in Reinforced Concrete Beams," U. S. Naval Civil Engineering Laboratory, Technical Report R 371, June, 1965.

BIBLIOGRAPHY

1. Baker, A. L. L., "A Plastic Theory of Design for Ordinary Reinforced and Prestressed Concrete Including Moment Re-Distribution in Continuous Members," Magazine of Concrete Research, No. 2, June, 1949, Pages 57-66.

2. Barnard, P. R., "The Collapse of Reinforced Concrete Beams," Flexural Mechanics of Reinforced Concrete - Proceedings of the International Symposium, Miami, Florida, November 10-12, 1964, Pages 501-521.

3. Berwanger, Carl, "Limit Design by Successive Moment Distribution," Proceedings of the American Society of Civil Engineers, Volume 92, No. ST1, February, 1966, Pages 405-430.

4. Broms, Bengt B., "Stress Distribution, Crack Patterns, and Failure Mechanisms of Reinforced Concrete Members," Journal of the American Concrete Institute, Volume 61, No. 12, December, 1964, Pages 1535-1560.

5. Burnett, E., "Flexural Rigidity, Curvature and Rotation and Their Significance in Reinforced Concrete Design," Magazine of Concrete Research, Volume 16, No. 47, June, 1964, Pages 67-72.

6. Chan, W. W. L., "The Rotation of Reinforced Concrete Plastic Hinges at Ultimate Load," Magazine of Concrete Research, Volume 14, No. 41, July, 1962, Pages 63-71.

7. Chan, W. W. L., "The Ultimate Strength and Deformation

of Plastic Hinges in Reinforced Concrete Frameworks," Magazine of Concrete Research, Volume 7, No. 21, November, 1955, Pages 121-132.

8. Ernst, G. C., "Plastic Hinging at the Intersection of Beams and Colums," American Concrete Institute Journal, Volume 28, No. 12, June, 1957, Pages 1119-1144.

9. Ernst, G. C., "Ultimate Slopes and Deflection--A Brief for Limit Design," Proceedings ASCE, Volume 81, No. 583, January, 1955.

10. Evans, R. H., "The Plastic Theories for the Ultimate Strength of Reinforced Concrete Beams," Journal of the Institute of Civil Engineers, No. 2, December, 1943, Pages 98-121.

11. Lee, L. H. N., "Inelastic Behavior of Reinforced Concrete Members Subjected to Short-Time Static Loads," Proceedings ASCE, Volume 79, Separate No. 286, September, 1953.

12. Mattock, A. H., "Rotational Capacity of Hinging Regions in Reinforced Concrete Beams," Flexural Mechanics of Reinforced Concrete - Proceedings of the International Symposium, Miami, Florida, November 10-12, 1964, Pages 143-182.

13. Nordell, W. J., "Plastic Hinge Formation in Reinforced Concrete Beams," U. S. Naval Civil Engineering Laboratory, Technical Report R 371, June, 1965.

14. Pfrang, E. O.; Siess, C. P.; Sozen, M. A., "Load-Moment-Curvature Characteristics of Reinforced Concrete Cross

Sections," Journal of the American Concrete Institute, July, 1964, Volume 61, No. 7, Pages 763-778.

15. Rosenblueth, Emilio; Diaz de Cossio, Roger, "Instability Consideration in Limit Design of Concrete Frames," Flexural Mechanics of Reinforced Concrete - Proceedings of the International Symposium, Miami, Florida, November 10-12, 1964, Pages 439-463.

16. Sawyer, H. A., Jr., "Design of Concrete Frames for Two Failure Stages," Flexural Mechanics of Reinforced Concrete - Proceedings of the International Symposium, Miami, Florida, November 10-12, 1964, Pages 405-439.

17. Sawyer, H. A., Jr., "Elastic-Plastic Design of Single Span Beams and Frames," Proceedings ASCE, Volume 81, No. 851, December, 1955.

18. Sawyer, H. A., Jr., "Status and Potentialities of Non-Linear Design of Concrete Frames," Flexural Mechanics of Reinforced Concrete - Proceedings of the International Symposium, Miami, Florida, November 10-12, 1964, Pages 7-28.

19. Wright, D. T.; Berwanger, Carl, "Limit Design of Reinforced Concrete Beams," Journal of the Structural Division ASCE, Volume 86, No. ST7, Paper 2541, July, 1960, Pages 1-36.

The vita has been removed from the scanned document

APPENDIX A

Tables for Rotation Calculations

TABLE 2.

ROTATION CALCULATIONS FOR BEAM NO. 1

AT

RIGHT

LOAD (KIPS)	MOMENT (KIP-IN.)	ROTATION (RAD/IN.)	DEPTH TO NA (INCHES)	STRAIN (1/IN.)
0.25	10.	0.00000	0.00	0.00000
0.83	24.	-0.41667	8.40	0.00006
1.20	32.	-0.08333	6.00	-0.00001
2.50	64.	0.25000	6.00	0.00003
2.45	63.	1.91667	5.48	0.00029
2.82	71.	1.75000	6.86	0.00003
2.82	71.	3.08333	5.84	0.00036
3.50	88.	4.41667	5.89	0.00049
3.50	88.	5.25000	5.71	0.00068
3.55	89.	5.66667	5.74	0.00072
3.71	93.	6.08333	6.08	0.00056
3.71	93.	7.41667	5.87	0.00084
3.71	93.	7.50000	6.33	0.00050
3.76	94.	10.08333	6.10	0.00091
3.97	99.	13.25000	6.19	0.00108
4.07	101.	15.66667	6.22	0.00122
4.07	101.	19.16667	6.26	0.00142
4.07	101.	24.16667	6.04	0.00232
4.07	101.	32.41667	5.97	0.00334
4.13	103.	39.58333	6.09	0.00361
4.07	101.	46.83333	6.13	0.00408
4.18	104.	56.83333	5.98	0.00578
4.23	105.	64.16667	6.03	0.00622
4.18	104.	71.08333	6.02	0.00696
4.23	105.	83.33333	5.95	0.00873

NOTE - ROTATION VALUES SHOWN HAVE BEEN MULTIPLIED BY 10**3.

TABLE 3.

ROTATION CALCULATIONS FOR BEAM NO. 1

AT

CENTER

LOAD (KIPS)	MOMENT (KIP-IN.)	ROTATION (RAD/IN.)	DEPTH TO NA (INCHES)	STRAIN (1/IN.)	DEFLECTION (INCHES)
0.37	13.	0.00000	0.00	0.00000	0.000
1.17	36.	0.50000	3.00	0.00015	0.016
1.91	63.	1.33333	-0.38	-0.00005	0.058
2.81	73.	1.91667	0.78	0.00015	0.092
3.45	99.	2.66667	0.75	0.00020	0.138
3.77	108.	2.41667	0.83	0.00020	0.152
4.03	119.	3.25000	0.77	0.00025	0.173
4.51	131.	3.33333	1.50	0.00050	0.198
4.77	142.	3.83333	1.17	0.00045	0.221
5.04	153.	4.75000	1.16	0.00055	0.242
5.41	168.	4.33333	1.38	0.00060	0.281
5.78	185.	4.50000	1.44	0.00065	0.316
6.05	198.	4.91667	1.53	0.00075	0.351
6.31	208.	7.91667	1.14	0.00090	0.437
6.47	212.	10.83333	0.97	0.00105	0.510
6.63	219.	14.91667	0.91	0.00135	0.617
6.68	220.	21.66667	0.83	0.00180	0.772
6.79	224.	28.08333	0.77	0.00215	0.957
6.79	225.	38.08333	0.79	0.00300	1.257
6.58	227.	41.16667	0.89	0.00365	1.585
7.05	238.	45.00000	0.97	0.00435	1.918
7.05	236.	47.75000	1.07	0.00510	2.255
7.48	254.	51.83333	1.12	0.00580	2.614
7.43	252.	55.91667	1.18	0.00660	2.889
7.43	252.	61.25000	1.33	0.00815	3.320

NOTE - ROTATION VALUES SHOWN HAVE BEEN MULTIPLIED BY 10**3.

TABLE 4.

ROTATION CALCULATIONS FOR BEAM NO. 1

AT

LEFT

LOAD (KIPS)	MOMENT (KIP-IN.)	ROTATION (RAD/IN.)	DEPTH TO NA (INCHES)	STRAIN (1/IN.)
0.41	14.	0.00000	0.00	0.00000
1.01	28.	0.41667	7.20	-0.00001
1.33	36.	0.33333	6.00	0.00003
2.68	68.	3.83333	5.61	0.00053
3.06	77.	4.50000	6.00	0.00045
3.17	80.	4.83333	5.79	0.00058
3.28	82.	5.33333	5.44	0.00083
3.49	88.	5.66667	5.91	0.00062
3.60	90.	6.25000	5.68	0.00083
3.66	91.	6.75000	5.93	0.00073
3.76	94.	7.41667	6.13	0.00064
3.76	94.	8.91667	5.89	0.00099
3.76	94.	9.58333	6.10	0.00086
3.87	97.	12.16667	6.00	0.00122
3.93	98.	13.33333	6.19	0.00108
3.93	98.	15.75000	6.13	0.00138
4.04	101.	19.50000	6.15	0.00165
4.09	102.	24.25000	6.16	0.00203
4.04	101.	32.75000	6.05	0.00313
3.01	76.	37.58333	6.15	0.00321
3.98	99.	45.58333	6.08	0.00421
4.04	101.	53.83333	6.05	0.00513
4.14	103.	62.25000	6.06	0.00588
4.20	104.	69.41667	6.04	0.00669
4.14	103.	78.75000	6.01	0.00778

NOTE - ROTATION VALUES SHOWN HAVE BEEN MULTIPLIED BY 10**3.

TABLE 5.

ROTATION CALCULATIONS FOR BEAM NO. 2

AT

RIGHT

LOAD (KIPS)	MOMENT (KIP-IN.)	ROTATION (RAD/IN.)	DEPTH TO NA (INCHES)	STRAIN (1/IN.)
0.36	12.	0.00000	0.00	0.00000
0.99	27.	-0.58942	-0.85	-0.00046
1.72	45.	-0.67363	2.97	-0.00027
2.66	68.	0.25261	9.90	-0.00007
2.66	68.	1.76827	6.79	0.00004
3.29	83.	3.11553	6.10	0.00028
3.39	85.	3.70495	6.21	0.00029
3.66	91.	4.63119	5.72	0.00059
3.92	98.	5.38902	5.38	0.00087
4.13	103.	5.30482	5.94	0.00056
4.65	115.	6.82048	5.57	0.00097
5.02	124.	7.15729	5.73	0.00091
5.02	124.	7.40990	5.74	0.00094
5.85	144.	8.33614	6.06	0.00079
6.06	149.	11.19906	5.80	0.00134
6.17	152.	13.64096	5.97	0.00140
6.22	153.	15.99865	5.97	0.00165
6.32	155.	20.37723	5.89	0.00226
6.38	157.	25.93466	5.86	0.00295
6.43	158.	30.31324	5.97	0.00312
6.48	159.	36.54429	5.86	0.00418
5.02	124.	41.42809	5.94	0.00440
6.69	164.	47.82755	5.95	0.00503
5.38	133.	52.96396	5.95	0.00557
6.59	162.	57.51095	5.91	0.00626

NOTE - ROTATION VALUES SHOWN HAVE BEEN MULTIPLIED BY 10**3.

TABLE 6.

ROTATION CALCULATIONS FOR BEAM NO. 2

AT

CENTER

LOAD (KIPS)	MOMENT (KIP-IN.)	ROTATION (RAD/IN.)	DEPTH TO NA (INCHES)	STRAIN (1/IN.)	DEFLECTION (INCHES)
0.27	8.	0.00000	0.00	0.00000	0.000
1.28	31.	1.17885	0.85	0.00010	0.019
1.91	49.	0.75783	-0.66	-0.00005	0.038
2.81	72.	1.34725	0.00	0.00000	0.079
3.50	100.	1.76827	-0.28	-0.00005	0.131
3.93	108.	2.02088	0.00	0.00000	0.143
4.09	112.	2.94712	0.85	0.00025	0.152
4.46	120.	2.52610	-0.20	-0.00005	0.165
4.88	132.	3.28393	1.22	0.00040	0.186
5.20	142.	3.53654	1.13	0.00040	0.192
5.62	153.	2.44190	0.00	0.00000	0.213
5.94	161.	3.36814	1.04	0.00035	0.227
6.15	166.	2.86292	1.75	0.00050	0.245
6.63	176.	3.78915	1.45	0.00055	0.271
7.00	179.	7.57831	0.99	0.00075	0.341
7.00	193.	13.55675	0.92	0.00125	0.481
7.11	191.	18.77737	0.80	0.00150	0.600
7.43	195.	26.18727	0.78	0.00205	0.740
7.53	202.	34.52341	0.62	0.00215	0.951
7.64	204.	39.91243	0.73	0.00290	1.151
7.80	210.	41.09128	0.86	0.00355	1.361
6.95	211.	44.96463	0.85	0.00380	1.685
7.27	216.	47.82755	0.92	0.00440	1.919
7.69	216.	51.36410	0.98	0.00505	2.219
7.90	226.	53.89020	1.00	0.00540	2.422

NOTE - ROTATION VALUES SHOWN HAVE BEEN MULTIPLIED BY 10**3.

TABLE 7.

ROTATION CALCULATIONS FOR BEAM NO. 2

AT

LEFT

LOAD (KIPS)	MOMENT (KIP-IN.)	ROTATION (RAD/IN.)	DEPTH TO NA (INCHES)	STRAIN (1/IN.)
0.30	11.	0.00000	0.00	0.00000
1.71	45.	0.67363	7.42	-0.00003
1.93	50.	0.50522	7.92	-0.00005
2.58	65.	3.03132	5.77	0.00037
3.01	76.	3.95756	5.81	0.00047
3.39	85.	3.95756	5.81	0.00047
3.55	89.	5.05221	5.34	0.00084
4.04	101.	6.39946	5.31	0.00108
4.41	110.	7.49411	5.60	0.00105
4.63	115.	8.08353	5.38	0.00131
4.90	121.	8.58875	5.65	0.00116
5.12	126.	9.59919	5.57	0.00137
5.50	136.	10.77804	5.47	0.00164
5.71	141.	12.37790	5.57	0.00176
6.74	165.	19.70360	5.73	0.00249
5.44	134.	19.95621	5.86	0.00227
5.98	147.	20.71405	5.84	0.00240
6.79	167.	28.03974	5.88	0.00313
6.58	162.	33.00775	5.85	0.00381
6.74	165.	38.90199	5.78	0.00473
6.79	167.	43.61738	5.85	0.00503
4.85	120.	46.81711	5.94	0.00497
4.04	101.	54.56383	5.91	0.00594
6.96	171.	64.58403	5.83	0.00756
5.77	142.	68.79421	5.84	0.00796

NOTE - ROTATION VALUES SHOWN HAVE BEEN MULTIPLIED BY 10**3.

TABLE 8.

ROTATION CALCULATIONS FOR BEAM NO. 3

AT

RIGHT

LOAD (KIPS)	MOMENT (KIP-IN.)	ROTATION (RAD/IN.)	DEPTH TO NA (INCHES)	STRAIN (1/IN.)
0.25	10.	0.00000	0.00	0.00000
0.93	26.	-0.38298	-1.31	-0.00032
1.82	47.	0.21277	17.63	-0.00023
2.19	56.	1.31915	7.01	-0.00000
2.71	69.	2.38298	5.56	0.00034
3.03	76.	2.97872	5.37	0.00049
3.66	91.	3.10638	5.88	0.00035
3.81	95.	4.00000	5.50	0.00060
4.44	110.	4.80851	5.88	0.00054
4.70	117.	6.12766	5.55	0.00089
6.01	148.	7.78723	5.71	0.00100
6.64	163.	8.55319	5.55	0.00124
7.58	186.	10.55319	5.45	0.00164
8.16	199.	11.65957	5.45	0.00181
8.52	208.	18.21277	5.71	0.00235
8.31	203.	24.42553	5.73	0.00310
8.31	203.	34.97872	5.67	0.00464
7.58	186.	41.53191	5.74	0.00522
7.63	187.	47.06383	5.75	0.00589

NOTE - ROTATION VALUES SHOWN HAVE BEEN MULTIPLIED BY 10**3.

TABLE 9.

ROTATION CALCULATIONS FOR BEAM NO. 3

AT

CENTER

LOAD (KIPS)	MOMENT (KIP-IN.)	ROTATION (RAD/IN.)	DEPTH TO NA (INCHES)	STRAIN (1/IN.)	DEFLECTION (INCHES)
0.37	14.	0.00000	0.00	0.00000	0.000
1.59	52.	0.97872	-0.77	-0.00007	0.044
2.60	64.	1.23404	-0.61	-0.00007	0.072
3.29	87.	2.25532	1.11	0.00025	0.111
4.35	123.	2.51064	0.80	0.00020	0.182
4.77	136.	2.55319	0.20	0.00005	0.209
5.09	139.	3.10638	0.72	0.00022	0.225
5.46	153.	2.93617	1.28	0.00037	0.243
5.99	166.	3.31915	1.36	0.00045	0.286
6.21	167.	5.70213	1.14	0.00065	0.332
6.89	172.	9.95745	0.78	0.00078	0.438
7.21	175.	13.78723	0.78	0.00107	0.525
7.58	175.	19.70213	0.77	0.00152	0.644
7.96	183.	22.68085	0.83	0.00188	0.723
8.17	185.	30.08511	0.74	0.00223	0.933
8.22	192.	34.76596	0.86	0.00297	1.188
8.27	196.	42.17021	0.91	0.00382	1.597
8.27	206.	47.70213	1.01	0.00482	1.963
8.11	207.	52.97872	1.04	0.00552	2.296

NOTE - ROTATION VALUES SHOWN HAVE BEEN MULTIPLIED BY 10**3.

TABLE 10.

ROTATION CALCULATIONS FOR BEAM NO. 3

AT

LEFT

LOAD (KIPS)	MOMENT (KIP-IN.)	ROTATION (RAD/IN.)	DEPTH TO NA (INCHES)	STRAIN (1/IN.)
0.30	11.	0.00000	0.00	0.00000
1.17	32.	0.00000	0.00	0.00000
3.17	80.	3.23404	5.80	0.00039
3.55	89.	4.42553	5.54	0.00065
4.14	103.	5.78723	5.23	0.00103
4.41	110.	6.68085	5.16	0.00123
4.74	117.	7.27660	5.36	0.00119
4.90	121.	7.57447	5.21	0.00135
5.17	128.	8.21277	5.57	0.00117
5.71	141.	9.65957	5.36	0.00159
6.63	163.	12.04255	5.34	0.00200
7.01	172.	12.93617	5.39	0.00208
7.44	182.	15.06383	5.28	0.00259
7.66	187.	15.91489	5.31	0.00269
7.98	195.	20.68085	5.44	0.00323
7.77	190.	26.21277	5.46	0.00405
7.66	187.	36.00000	5.44	0.00560
7.60	186.	44.00000	5.39	0.00710
6.85	168.	50.46808	5.25	0.00883

NOTE - ROTATION VALUES SHOWN HAVE BEEN MULTIPLIED BY 10**3.

APPENDIX B

Computer Program

```
$ID   MURRAY, KENNETH H.  CONCRETE BEAM C. E. DEPT.
$IBJOB
$IBFTC
C      A = DISTANCE OF RIGHT CANTILEVER  (INCHES)
C      B = DISTANCE BETWEEN FIRST LOAD AND SUPPORT (INCHES)
C      C = DISTANCE BETWEEN FIRST LOAD AND CENTER LOAD
C          (INCHES)
C          (INCHES)
C      I = NUMBER OF READING
C      M = TOTAL NO. OF READINGS
C      G = DISTANCE OF LEFT  CANTILEVER (INCHES)
C      DEPTH = DISTANCE BETWEEN STRAIN POINTS (VERTICAL
C                INCHES)
C      E = DISTANCE BETWEEN THIRD  LOAD AND LEFT SUPPORT
C          (INCHES)
C      P(I)    = CENTER LOADS (KIPS)
C      PSI(1,I) = CENTER LOADS (PSI)
C      P1(I)     = RIGHT LOAD (KIPS)
C      D = DISTANCE BETWEEN CENTER LOAD AND THIRD LOAD
C      PSI(2,I) = RIGHT LOAD (PSI)
C      PSI(3,I) = LEFT LOAD (PSI)
C      P2(I)     = LEFT LOAD (KIPS)
C      RL(I) = LEFT SUPPORT REACTION (KIPS)
C      SRM(I) = MOMENT AT RIGHT SUPPORT (KIP - INCHES)
C      SLM(I) = MOMENT AT LEFT SUPPORT (KIP - INCHES)
```

```
C     CLM(I) = MOMENT AT CENTER CORRECTED FOR BEARING
C              PLATE WIDTH (KIP - INCHES)
C     S(J,I) = STRAIN GAGE READING ( J = NO. OF POINT)
C     SI(J)  = STRAIN GAGE READING INITIALLY (J = SAME)
C     ROTRT(I) = ROTATION AT RIGHT SUPPORT (RAD/IN. X .001)
C     ROTLT(I) = ROTATION AT  LEFT SUPPORT (RAD/IN. X .001)
C     ROTCL(I) = ROTATION AT CENTER LINE   (RAD/IN. X .001)
C     J = 1 AT CENTER
C     J = 2 AT RIGHT
C     J = 3 AT LEFT
C     CONST(J,I) = CONCRETE STRAIN (1/IN.)
C     DEFL(I) = DEFLECTION AT CENTER (INCHES)
C     TOPST(J,I) = STRAIN AT TOP
C     BOTST(J,I) = STRAIN AT BOTTOM
C     CNA(J,I) = DISTANCE FROM TOP TO NEUTRAL AXIS
C                (INCHES)
      DIMENSION S(12,30),SI(12),P(30),P1(30),P2(30),
     1PSI(3,30),RL(30),SLM(30),SRM(30),CLM(30),ROTLT(30),
     2ROTRT(30),ROTCL(30),CNA(3,30),TOPST(3,30),BOTST(3,30)
     3 ,DEFL(30) , CONST(3,30)
      READ (5,10) A,B,C,D,E,G,DEPTH,M
   10 FORMAT (6F4.1,F6.4,I2)
      READ (5,20) SI
      READ (5,20)((S(J,I),J =1,12),I =2,M)
   20 FORMAT (12F5.1)
```

```
      READ (5,30) ((PSI(J,I),J=1,3),I=1,M)
   30 FORMAT (3F5.1)
      READ (5,31) (DEFL(I), I = 1,M)
   31 FORMAT (10F6.4/10F6.4/5F6.4)
      ROTCL(1) = 0.0
      ROTRT(1) = 0.0
      ROTLT(1) = 0.0
      WRITE (7,40)
   40 FORMAT(    10X,36HROTATION CALCULATIONS FOR BEAM NO. 1
     1//28X,2HAT,//)
      DO 50  I = 1,M
      P(I) = (10.603*PSI(1,I) - 50.0)*0.001
      P1(I)= (10.465*PSI(2,I) - 60.0)*0.001
      P2(I)= (10.814*PSI(3,I) - 20.0)*0.001
      RL(I) = (P2(I)*(B+C+D+E+G)+P(I)*(3.0*B+2.0*C+D)
     1 - P1(I)*A)/96.0
      SLM(I) = P2(I)*G + 3.67
      SRM(I) = P1(I)*A + 3.67
   50 CLM(I) =(RL(I)*(E+D) - P2(I)*(G+E+D) - P(I)*D + 3.08)
     1 -P(I)
      Q = DEPTH*2.0
      DO 56 I = 2,M
      TOPST(1,I) = S(5,I)-SI(5)+S(7,I)-SI(7)
      BOTST(1,I) = SI(6)-S(6,I)+SI(8)-S(8,I)
      TOPST(2,I) = SI(1)+SI(3)-S(1,I)-S(3,I)
```

```
      BOTST(2,I) = S(2,I)+S(4,I)-SI(2)-SI(4)
      TOPST(3,I) = SI(9)+SI(11)-S(9,I)-S(11,I)
      BOTST(3,I) = S(10,I)+S(12,I)-SI(10)-SI(12)
      ROTRT(I) = (TOPST(2,I)+BOTST(2,I))/Q
      ROTCL(I) = (TOPST(1,I)+BOTST(1,I))/Q
      ROTLT(I) = (TOPST(3,I)+BOTST(3,I))/Q
      DO 53 J = 1,3
      IF (TOPST(J,I)+BOTST(J,I)) 51,52,51
   51 CNA(J,I) = TOPST(J,I)*DEPTH/(TOPST(J,I)+BOTST(J,I))
      GO TO 53
   52 CNA(K,I) = 0.000
   53 CONST(J,1) = 0.0
      CONST(1,I) = TOPST(1,I) *0.00005
      DO 56 J = 2,3
      IF (CNA(J,I)) 54,55,54
   54 CONST(J,I) =(TOPST(J,I)*(7.0-CNA(J,I))/CNA(J,I))
     1  *0.00005
      GO TO 56
   55 CONST(J,I) = 0.0
   56 CONTINUE
      WRITE (7,60)
   60 FORMAT (26X,5H LEFT//2X,4HLOAD, 6X,6HMOMENT,7X,
     1 8HROTATION,4X,11HDEPTH TO NA,5X,6HSTRAIN/7H (KIPS),3X
     2 , 9H(KIP-IN.),5X,9H(RAD/IN.),5X,8H(INCHES),6X,
     3 7H(1/IN.))
```

```
      DO 70 I = 1,M
   70 WRITE (7,71) P2(I),SLM(I),ROTLT(I),CNA(3,I),CONST(3,I)
   71 FORMAT (F6.2,7X,F4.0,7X,F8.5,7X,F5.2,7X,F8.5)
      WRITE (7,40)
      WRITE (7,80)
   80 FORMAT (26X,5HRIGHT//2X,4HLOAD, 6X,6HMOMENT,7X,
     1 8HROTATION,4X,11HDEPTH TO NA,5X,6HSTRAIN/7H (KIPS),3X
     2 , 9H(KIP-IN.),5X,9H(RAD/IN.),5X,8H(INCHES),6X,
     3 7H(1/IN.))
      DO 90 I = 1,M
   90 WRITE (7,71) P1(I),SRM(I),ROTRT(I),CNA(2,I),CONST(2,I)
      WRITE (7,40)
      WRITE (7,100)
  100 FORMAT (26X,6HCENTER//2X,4HLOAD,3X,6HMOMENT,4X,
     1 8HROTATION,2X,11HDEPTH TO NA,2X,6HSTRAIN,2X
     210HDEFLECTION/7H (KIPS),1X,9H(KIP-IN.),2X,
     3 9H(RAD/IN.),3X,8H(INCHES),3X,7H(1/IN.),2X,8H(INCHES))
      DO 110 I = 1,M
  110 WRITE (7,111) P(I),CLM(I),ROTCL(I),CNA(1,I),
     1 CONST(1,I), DEFL(I)
  111 FORMAT (F6.2,3X,F4.0,6X,F8.5,4X,F5.2,5X,F8.5,3X,F5.3)
  120 STOP
      END
$ENTRY
      DATA DECK
$IBSYS
```

Experimental Studies on the Limit Analysis of Reinforced Concrete Fixed-Ended T-Beams

By

Kenneth Harold Murray

ABSTRACT

Results are presented on tests of reinforced concrete T-beams with a flange 20 inches wide by two inches thick setting on a stem five inches deep and four inches wide. These beams were loaded at the quarter points of an eight-foot span and also at the end of cantilever sections of two feet. The beams were loaded until they collapsed. The reinforcing steel was varied at the support section, but remained constant at the center.

Moment-curvature information is developed from the experimental results, and conclusions are drawn concerning present theory for deriving analytical moment-curvature relationships for reinforced concrete sections. Ultimate concrete strain in confined sections is reviewed in light of the experimental results.

Discussed also are current theories for calculating ultimate loads for indeterminate reinforced concrete beams.